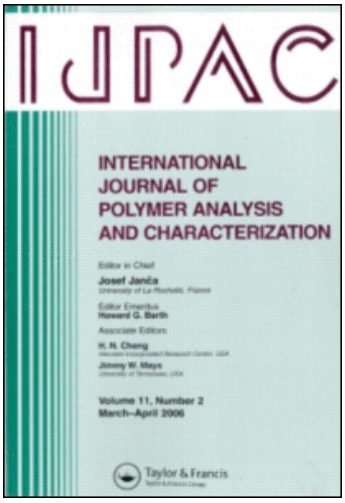

International Journal of Polymer Analysis and Characterization
Publication details, including instructions for authors and subscription information:
http://www.informaworld.com/smpp/title~content=t713646643

Simulation of Molecular Weight Distributions of Poly(N-[10-(n-docosane[oxycarbonyl])-n-decyl maleimide]) from Isothermal Fractional Precipitation Data and Comparison with Distributions from Size Exclusion Chromatography of Fractions

E. Carazo Chico[a]; J. M. Barrales-Rienda[a]
[a] Departamento de Química-Física de Polímeros, Instituto de Ciencia y Tecnología de Polímeros, Spain

Online publication date: 27 October 2010

To cite this Article Chico, E. Carazo and Barrales-Rienda, J. M.(2003) 'Simulation of Molecular Weight Distributions of Poly(N-[10-(n-docosane[oxycarbonyl])-n-decyl maleimide]) from Isothermal Fractional Precipitation Data and Comparison with Distributions from Size Exclusion Chromatography of Fractions', International Journal of Polymer Analysis and Characterization, 8: 2, 99 — 132
To link to this Article: DOI: 10.1080/10236660304889
URL: http://dx.doi.org/10.1080/10236660304889

International Journal of Polymer Anal. Charact., 8: 99–132, 2003

1023-666X/03 $12.00 + .00
DOI: 10.1080/10236660390128319

Taylor & Francis
Taylor & Francis Group

Simulation of Molecular Weight Distributions of Poly (N-[10-(n-docosane[oxycarbonyl])-n-decyl maleimide]) from Isothermal Fractional Precipitation Data and Comparison with Distributions from Size Exclusion Chromatography of Fractions

E. Carazo Chico and J. M. Barrales-Rienda
Departamento de Química-Física de Polímeros,
Instituto de Ciencia y Tecnología de Polímeros, Spain

Twenty fractions of an unfractionated sample of poly(N-[10-(n-docosane[oxycarbonyl])-n-decyl)maleimide]) (PEMI 10-22) were obtained by isothermal fractional precipitation at 25°C using toluene/methanol as the solvent/precipitant system. Weight-average molecular weights (in the range $\bar{M}_w = 6.06 \times 10^3$ to 3.21×10^5) of 11 of these fractions were measured by static light scattering. The molecular weight distribution (MWD) of PEMI 10-22 was analyzed by comparing the results obtained from isothermal fractional precipitation with size exclusion chromatography (SEC). The analysis of SEC data was carried out by means of a nonlinear autocalibration of log $\bar{M}_w$ versus elution time at the peak, t_e(peak). The calibration was determined by an iterative computer method devised for use with polydisperse samples. The results of isothermal fractional precipitation are simulated and compared with SEC data. Good agreement between the distribution determined by the SEC autocalibration method and isothermal fractional precipitation was obtained.

Received 20 July 2001; accepted 26 November 2001.
This work was partially funded by the DCICYT through Grants PB 92-0773-03-1 and PB 95-0134-002-00.
Address correspondence to J. M. Barrales-Rienda, Departamento de Química-Física de Polímeros, Instituto de Ciencia y Tecnología de Polímeros, C.S.I.C. Juan de la Cierva, 3, E-28006, Madrid, Spain. E-mail: jmbarrales@ictp.csic.es

Keywords: Poly(*N*-[10-(*n*-docosane[oxycarbonyl])-*n*-decyl maleimide]); Isothermal fractional precipitation; Size exclusion chromatography; Autocalibration; Molecular weight distribution; Simulation

A major problem of comb-like polymers such as poly *N*-maleimides arises from the fact that they have a broad molecular weight distribution. If one wishes to study, for instance, the influence of main chain length on the crystallization behavior, it is thus necessary to fractionate these polymers.

Fractional precipitation, coacervate extraction, and fractionation by crystallization are all methods of batch fractionation[1]. The separation is achieved by the partition of the polymer between two immiscible phases. Several days are usually required to obtain the cuts. The cuts then must be further analyzed. Thirty years ago batch fractionation methods were commonly used for analytical fractionation. Because of the simplicity in experimental equipment and technique, these methods are still used today for preparative fractionation[2,3]. In Cantow's and Tung's books the methods of batch fractionation are discussed in chapters by Kotera[4], Elliot[5], and Kamide[6]. The partition of polymers in two immiscible phases is governed by the thermodynamics of polymer solutions, and background on these theories can be found in most polymer chemistry books. In Cantow's book these theories were surveyed by Huggins and Okamoto[7] and later by Huggins[8].

Most of the studies published so far have been done mainly with analytical fractionation, where the molecular weight distribution (MWD) of the original sample is evaluated using data of the fraction size ρ and one of its molecular weight averages ($\bar{M}_n$, $\bar{M}_v$, or $\bar{M}_w$). Thirty years ago, Kamide et al.[9] and Koningsveld and Staverman[10,11] formulated a rigorous theory of fractionation in which the initial concentration, namely, the polymer volume fraction in the solution v_p^0 and the relative amount or size of the fraction ρ are given in advance[12].

Molecular weight distribution (MWD) and statistical molecular weight averages are possible from size exclusion chromatography (SEC) measurements[13,14] with the use of: (1) an on-line light-scattering detector without column calibration; (2) an on-line viscometer with universal calibration; or (3) with proper column calibration (i.e., autocalibration). The use of SEC in combination with viscometry and light scattering (LS) detectors for estimation of the absolute molecular weight distribution is common. Multiple detector SEC is especially useful for characterizing very complex polymeric materials such as copolymers, blends, and branched polymers. However, to generate reproducible results on a routine basis, special care must be taken regarding the added complexity and costs of the instrumentation. In particular, detector configuration should be chosen carefully, interdetector volumes (dead volumes)

measured precisely, concentration-detector response calibrated, baseline settings and instrument sensitivity parameters selected with care, and band-broadening corrections used if needed. Finally, to verify the accuracy of a multiple-detector SEC system, the instrument must be evaluated using well-characterized standards[15–18].

Some possible solutions to avoid these difficulties have been given by Jackson and Barth[15]. However, there exist real and, in some cases, serious limitations of these detection systems for analyzing low molecular weight polymers ($<5.0 \times 10^4$). Viscometry and LS detectors are not as sensitive to lower molecular weight polymers under normal SEC conditions. The concentration detector, which usually is a refractometer, does not always give reliable concentration response below 5.0×10^4 g/mol unless a meticulous calibration is done. The viscometer sensitivity is dependent upon the specific viscosity of each sample, so it is very common to compensate by using high concentrations for low molecular weight samples to get reliable signal/noise ratios. However, these high concentrations in turn influence the elution time/volume of the sample. Accurate elution volumes are critical for molecular weight determinations when SEC universal calibration is used. Sensitivity of an LS detector is a molecular weight function. With polymers below 2.5×10^4 g/mol, the sensitivity is a limitation. The signal from the LS detector is due to the sample's excess Rayleigh factor R_θ. The excess Rayleigh factor is a function of the square of the increment in refractive index with concentration ($[dn/dc]^2$). Therefore, if the sample exhibits a low dn/dc, less than 0.06 under normal SEC concentrations, the detector may not provide sufficient signal-to-noise to calculate the MWD. The dn/dc of low molecular weight samples is affected adversely by end groups. In other words, in the very low MW range, the detector is more sensitive to chemical composition than it is to MW. The refractive index detector response for low molecular weight concentration determinations can be unreliable because the dn/dc of the sample may change as a function of MW below 5.0×10^4 g/mol[19]. However this fact may be avoided by using adequate corrections.

Therefore, the sensitivity of the actual detectors is such that there is only a small range of sizes where the results of both techniques (viscometry and light scattering) are precise enough to be used simultaneously, and universal calibration is still in use in many laboratories[20]. This fact may be especially serious in the low molecular weight region, as the present system may be. Jackson and Barth[16] have critically described inherent problems in data analysis and possible potential sources of error and advantages and disadvantages of using SEC techniques and procedures.

Procházka and Kratochvil[21,22], however, by means of an analysis of the accuracy of determining molar-mass averages of polymers by gel permeation chromatography (GPC) with an on-line light-scattering detector demonstrated that, because of limited sensitivity of molar-mass

and concentration detectors, only M_w can be determined with acceptable accuracy by means of SEC with an on-line low-angle laser-light scattering (LALLS) photometer; $\bar{M}_n$ can be determined accurately only if the polydispersity of the analyzed sample is small. A somewhat more exact determination of $\bar{M}_n$ is possible using data of the concentration detector and calibration of the chromatographic column. The sensitivity of light scattering and viscosity detectors increases with molecular weight. As a result, these detectors give a high signal-to-noise ratio as compared to a concentration-sensitivity detector at the high molecular weight end of the distribution. At the low molecular weight end of the distribution, the situation is reversed[16]. Thus, often, the ends of the distribution are truncated, resulting in an underestimation of the sample polydispersity[21,22].

The measurement of molecular weight averages and the distribution for polymers by size exclusion chromatography (SEC) requires the construction of a calibration curve using polymers that are relatively monodisperse or have a very narrow distribution as standards. However, to calculate the molecular weight averages and the distribution for any polymers other than polystyrene (PS) by this calibration curve, it is necessary to transform molecular weight units in PS into those for the polymer specified.

Some attempts have been undertaken to overcome the problem of the lack of suitable standards for each polymer type[23–27]. In some cases a number of samples with a variety of molecular weights are used as standards. Some of the methods for calibration using polydisperse polymer samples were employed to prepare linear calibration curves[23–25]. However, it is very well known that a calibration curve of a given column may yield a logarithm plot of molecular weight against elution volume or time with a slight, but important, curvature in the molecular weight range where the data has to be evaluated. For this reason, the calibration curve should be fitted by third-order polynomial[28]. McCrackin[26] proposed a calibration method in which third-order polynomials are used.

A method of calibrating SEC columns using polydisperse polymer samples was developed by Balke et al.[23], but was applied only to linear calibration curves. Another calibration method was developed by Weiss and Cohn-Ginsberg[29] but requires the molecular weight distribution of the polymer samples used for calibration to be of a particular shape, so it is not generally applicable. The calibration curve is established from narrow distribution polystyrenes and then extended to other systems. Two polymers having different intrinsic viscosities or a polymer of known intrinsic viscosity and at least one average of the molecular weight are required to calculate the parameters of the SEC curves. This method has been validated by Morris[30]; Hamielec and Omorodin[31] improved this method. Mori[32] also presented a modification of the methods of

Weiss and Cohn-Ginsberg[29] and Hamielec and Omorodin[31] for calibrating SEC columns.

It is well established that the best results are obtained from SEC primary data, where the system of interest is analyzed using an autocalibration method, namely, calibration by means of standards of the same polymer[3,33,34]. This is especially true when non-exclusion effects are present[35]. Barth[36] reviewed "nonsize" exclusion effects and their detrimental effects on the molecular weight determination of polymers. Elution times t_e may be converted into molecular weights M only by means of correlation. This is possible only when a molecular weight average is known using a direct technique, and the elution time is viable only for monodisperse systems. However, since this does not seem to be the present case, it has been necessary to develop a calibration method of SEC using a number of polydisperse samples, ignoring any method applied based in the universal calibration. Since, so far, it is unknown whether this polymer obeys such a correlation, the universal concept cannot be used with any type of certainty.

From the above-mentioned reasons, automatic techniques seem to be adequate in the high molecular weight region or for quality control purposes. Nevertheless these circumstances do not apply in our samples because they are in the low $\bar{M}_w$ region; furthermore, we need to characterize not only the $\bar{M}_w$ average but other molecular averages like $\bar{M}_n$, which is much less precise as determined using the above-mentioned techniques.

Therefore, the main purpose of the present work is threefold. First, the analysis of fractionation data according to the Kamide theory has been applied only to data obtained by *fractional solution by temperature lowering*. However, in the present article we intend to apply the same theory to data obtained by *isothermal fractional precipitation*. Second, we seek to estimate more precise and realistic values of the molecular weight averages; and third, we will investigate the use of an autocalibration procedure for SEC to avoid secondary exclusion processes, which normally are not taken into account in the case where polystyrene standards are used.

EXPERIMENTAL

Polymer

The synthesis of the monomer *N*-(10-[*n*-docosane(oxycarbonyl)]-*n*-decyl)maleimide, its purification, and its polymerization can be found in a forthcoming paper[37]. Purification was achieved by two dissolution and precipitation steps followed by drying under high vacuum at 40°C (10^{-4} to 10^{-5} mm of Hg). The purified sample was characterized by organic

elemental analysis, ^{13}C- and ^{1}H-NMR techniques, and infrared (IR) spectroscopy to verify the chemical structure and purity of the sample.

Solvents

Analytical grade toluene and methanol (Panreac Monplet & Esteban, S.A. Barcelona, Spain) were dried, redistilled, and stored over a suitable desiccant agent and freshly distilled prior to use. Generous head and tail fractions were discarded. The SEC solvent was analytical grade tetrahydrofuran (THF) (Scharlau, Barcelona, Spain) purified by refluxing for at least 72 h over anhydrous potassium hydroxide under a nitrogen atmosphere and subsequently distilled on a rectification column. The boiling fraction at 66.5°C–67.0°C, with a corresponding refractive index[38] n_D (25°C) = 1.4049_6, was used. It was stabilized with 2,6-di-*tert*-butyl-4-methylphenol (BHT) to prevent the formation of peroxides.

Isothermal Fractional Precipitation

Toluene/methanol was employed as the solvent/precipitant system. The fractional precipitation was carried out using a conventional procedure, starting with a 1.912% toluene solution (41.1 g/2150 mL). Addition of the precipitant up to cloudiness was followed by dissolution and thermal reequilibration in a 5000 mL separation funnel in a thermostatic water bath at 25.0 ± 0.1°C. The fractions precipitated in a concentrated solution state. They were redissolved in toluene, precipitated with methanol, and subsequently dried at 40°C (10^{-4} to 10^{-5} mm Hg) for 24 h. The fractional precipitation data is given in Table I (columns 1–3), where W_i represents the weight in grams for each fraction. The fractionation yield was 98.5% (see Table I). It can be considered as satisfactory for our purposes, as will be seen subsequently. Twenty fractions were obtained.

Size Exclusion Chromatography

SEC experiments were performed on a Waters Associates gel permeation chromatograph composed of the following parts: a U6K Universal Liquid Chromatograph Injector, a Waters 600 E Multisolvent Delivery System, and an R-410 Differential Refractometer with tetrahydrofuran (THF) as mobile phase. The columns and detector were kept at 25°C by means of a circulating bath. The temperature of the circulating water bath for both columns and detector was maintained at approximately ±0.2°C. The circulating thermostat was a Haake Model F-35 (Karlsruhe, Germany). The temperature was monitored by means of a precision quartz Hewlett-Packard 2804A thermometer with a quartz

TABLE I Fractional precipitation data of poly(*N*-[10-(*n*-docosane[oxycarbonyl])-*n*-decyl maleimide]) PEMI 10-22. Fractionation yield = $(\Sigma W_i/W).100 = (40.4936/41.1).100 = 98.5\%$

Fraction number	$V(CH_3OH)$ added (mL)	$V(CH_3OH)$ accumulated (mL)	V_c (Precipitate volume) (mL)	W_i (g)	$c = W_i/V_c$ (g·mL^{-1})
F-1	625	625	9.1	1.5017	0.1650
F-2	15	640	15.4	2.6155	0.1698
F-3	78	718	11.6	1.9950	0.1727
F-4	13	731	9.5	1.6805	0.1769
F-5	15	746	11.7	2.1181	0.1810
F-6	17	763	14.9	2.8277	0.1898
F-7	14	777	9.4	1.7715	0.1885
F-8	15	792	11.6	2.2849	0.1978
F-9	15	807	11.6	2.2653	0.1961
F-10	28	835	11.1	2.3365	0.2103
F-11	24	859	9.3	2.0318	0.2185
F-12	20	879	6.6	1.4610	0.2214
F-13	27	906	7.4	1.6944	0.2290
F-14	36	942	8.0	1.8864	0.2358
F-15	46	988	7.5	1.8469	0.2463
F-16	80	1068	9.4	2.4728	0.2645
F-17	120	1188	6.3	1.7485	0.2775
F-18	190	1378	5.7	1.7995	0.3157
F-19	350	1728	6.0	2.1985	0.3664
F-20	60	1788	5.7	1.9571	0.3434

sound probe Model 18111A (Mountain View, Calif., USA). An arrangement of four columns in series was previously selected according to the molecular weight distribution of the unfractionated sample. It consists of four (122 cm [4 feet] long) Styragel columns with an external diameter of 0.9 cm (I.D. 7.8 mm), and upper porosity ratings of 10^3, 3×10^3, 10^4, and 10^5 Å (Waters designation). Samples were dissolved overnight at room temperature. The polymer solutions were prepared in the range of concentrations 0.2 to 0.3 wt%. Prior to the injection of the solutions, they were filtered through a 10 μm MF filter (Millipore).

Special attention had to be paid to the stability and accuracy of the SEC equipment. The following steps appeared to be effective:

(1) Determination of the column set efficiency. This was carried out by measuring the number of theoretical plates using *o*-dichlorobenzene (ODCB) as marker. Where tetrahydrofuran was the solvent, the columns yielded 11,600 theoretical plates, $t_e(ODCB) = 95.83$ min;

$\Delta t = 3.56$ min. This amounts to, for a set of four columns, 2900 plates/column. Column efficiency was checked twice a week and remained stable during the experiments.

(2) Selection of the appropriate set of chromatographic columns. This is an important task especially because this study involves fractionation by fractional precipitation, SEC, and fractional simulation. Finally the system was found to be at its optimum for a set of four columns. This selection was restricted by the availability of appropriate columns to obtain absolute molecular weight values of a series of fractionated samples with a wide molecular weight distributed over a determined wide range.

After the operation conditions were optimized, the experimental conditions were fixed as follows:

(*a*) Flow rate was 2.0 mL/min. At this flow rate "viscous fingering" does not occur. In the construction of a universal calibration curve using an on-line viscometer, or, as in our case using an average of the molecular weight, SEC concentration effects (macromolecular crowding and viscous fingering) must be absent[36]. Flow rates, measured volumetrically and tested volumetrically (by siphon) and gravimetrically (by balance), were maintained. For either the elution time, elution volume, or elution weight, measurements were taken at given time intervals. Time measurements gave the best accuracy and reproducibility.

(*b*) Sample concentration and the injection volume of the solution were 2.5 mg/mL and 2 mL, respectively; a 5 mL syringe was used.

(*c*) Pressure drop across the column set was approximately 260–300 psi at a flow rate of 2 mL/min and a temperature of 25°C.

(*d*) The flow rate of (purge) degasifying gas (He) was kept at 60 mL/min.

(*e*) In order to stabilize the baseline during the measurements, thus avoiding pressure overloading caused by the higher molecular weight polymer molecules, a set of two columns of 3×10^8 and 10^4 Å were located as back-pressure columns in the reference line.

(*f*) The flow was then adjusted to a ratio of 1:20 with respect to the sample line. This flow and splitting ratio were maintained during the course of the measurements and their stability checked.

(*g*) A detector gain of $\times 2$ was used. Run time: 120 min ($t_0 = 50$ min; $t_f = 100$ min). The baseline was optimized.

(*h*) Data acquisition and calculations on primary data were carried out on-line by means of a Baseline 810 Waters Data System (Waters Associates, Inc., Milford, Mass., USA). For the above experimental conditions, an SEC chromatogram was recorded for the whole polymer and can be seen in Figure 1. Similarly, the chromatograms were obtained for 20 fractions. Chromatograms of certain fractions are shown in Figure 2.

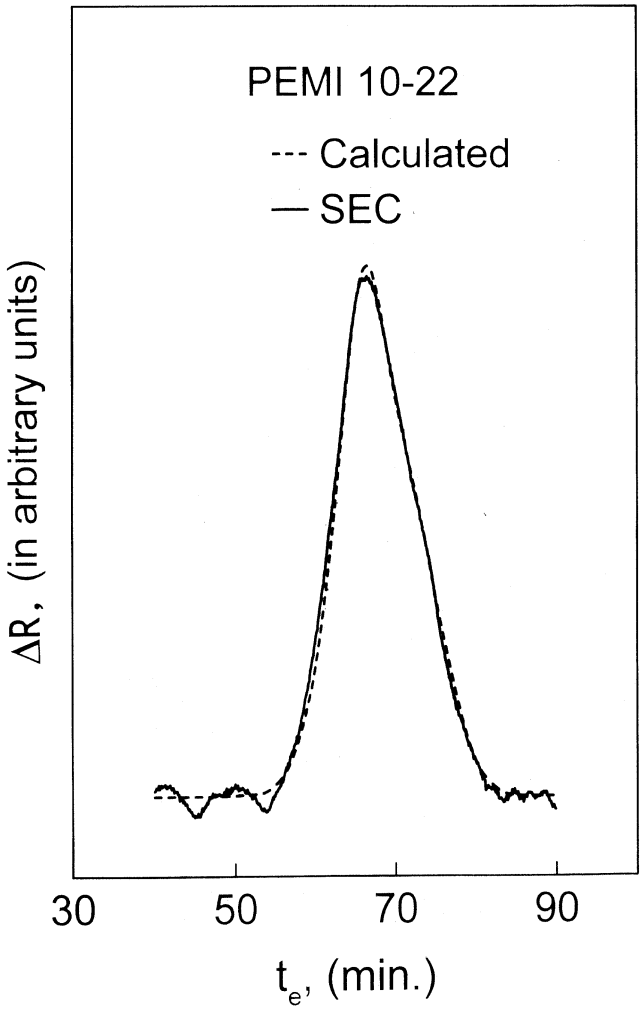

FIGURE 1 SEC chromatogram tracing of the complete PEMI 10-22 polymer sample. The experiment was carried out at 25°C and the eluent employed was THF. The dashed line corresponds to the corrected baseline chromatograms of PEMI 10-22 fractions F-1 to F-20. The curve was calculated from the individual SEC tracing of each of the fractions obtained by fractional precipitation.

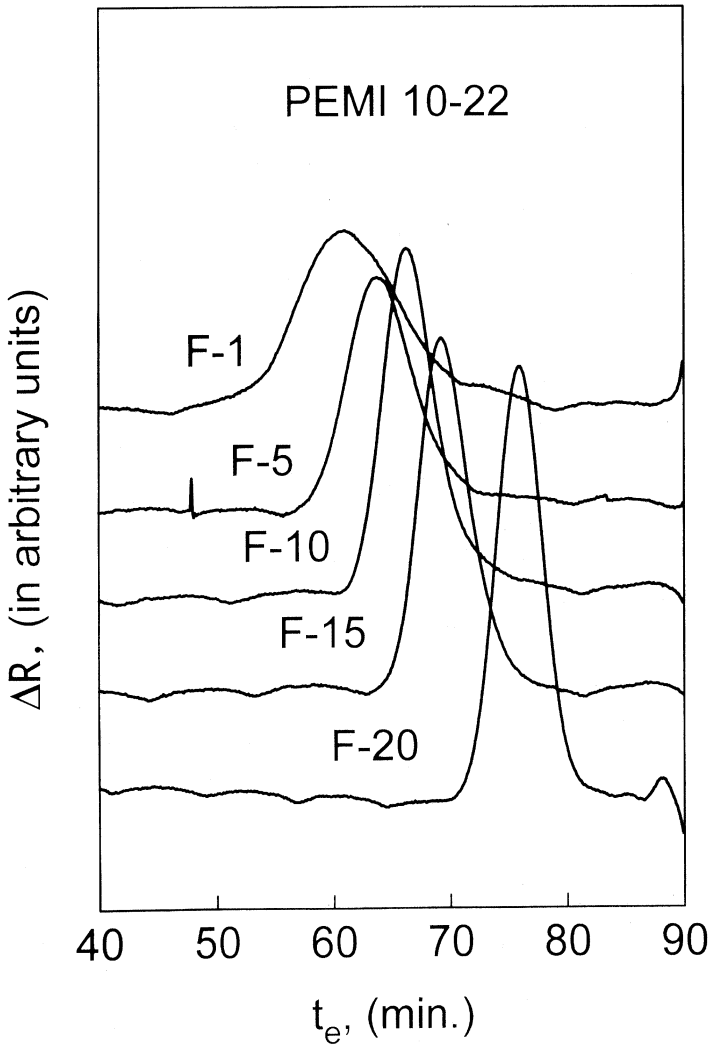

FIGURE 2 SEC tracings of fractions F-1, F-5, F-10, F-15, and F-20 employing the same experimental conditions used in Figure 1.

Refractive Index Increment Measurements

All chromatograms have been corrected for baseline and refractive index corrections due to molecular weight effects. The relationship between molecular weight and refractive index of a polymer is generally

assumed to be constant, independent of molecular weight for molecular weights above a few thousand. Sensitive refractive index measurements on solutions have indicated that they exhibit a small systematic molecular weight–refractive index dependence[39]. Refractive index shows significant variation with $\bar{M}_n$. It is generally linear in $1/\bar{M}_n$[40–43]. Carazo and Barrales-Rienda[37] have obtained a series of values of dn/dc for a series of fractions of poly(*N*-[10-(*n*-docosane[oxycarbonyl])-*n*-decyl maleimide]) covering a wide range of molecular weights. They depend on molecular weight and can be fitted to the following semiempirical expression:

$$dn/dc = b - (a/M) \tag{1}$$

which may be also expressed by means of its linearized form as

$$\log [b - (dn/dc)] = \log a - \log M \tag{2}$$

if we substitute the decimal logarithm of molecular weight by the elution volume (retention time), corresponding to the maximum of the curve obtained by SEC, since as we know they are practically proportional, namely,

$$\log M = C_o - Ct_e \tag{3}$$

Equation (2) may be also rewritten as

$$\log [b - (dn/dc)] = \log a - C_o + C_1 t_e = \log a' + C_1 t_e \tag{4}$$

The following parameters were obtained: $b = 0.08248$; $\log a' = -9.15961$, and $C_1 = 0.09326$ with a correlation coefficient of $R^2 = 0.999999$. These parameters were used to correct the dn/dc signal. Error in molecular weight caused by the variation in the refractive index increment at low molecular weights can lead to errors of 10–25% in the determination of the number-average molecular weight for polydisperse materials[44]. This last correction has been done by taking into account the molecular weight dependence of the refractive index increment, which was determined and employed previously[37] by means of a differential refractometer, since the direct consequence of small changes in the refractive index–molecular weight constant in the middle molecular weight range would affect molecular weights calculated from light-scattering measurements. The width of a peak in an SEC chromatogram is mainly due to three factors: the polydispersity of the sample, the column spreading, and the spreading produced by injecting the polymer sample in a finite volume of solvent. For samples with broad MWD, the spreading due to the polydispersity of the sample is much larger than the other components of the spreading, which may therefore be neglected as a first approximation, and the molecular weight averages $\bar{M}_w$ and $\bar{M}_n$ and the polydispersity $\bar{M}_w/\bar{M}_n$ may

be computed from the chromatogram[45]. No correction due to the band broadening or axial dispersion of the columns was applied due to the polydispersity factor range[3] of the present series of fractions.

As mentioned previously, Figure 2 shows a series of chromatograms corresponding to F-1, F-5, F-10, F-15, and F-20 fractions. In this series of chromatograms it can be observed how the successive fractions have narrower distribution (a less polydispersity factor) and appear at longer elution times (smaller molecular weights).

EXPERIMENTAL RESULTS

Analysis of SEC Data

To test the validity of this fractionation procedure using the following method, the SEC chromatogram corresponding to the whole polymer sample, i.e., the unfractionated sample, was reconstructed by means of the chromatograms from the different fractions. This result was then compared with the chromatogram that corresponded to the unfractionated sample. To do this, it is necessary to normalize the chromatograms for each of the isolated fractions, followed by subsequent addition using the statistical weight for each weight fraction obtained during the fractionation. The result of this treatment is shown as a dotted line in Figure 1. It can be observed that only a small difference exists between the chromatogram that corresponds to the whole sample and that reconstructed from the chromatogram and normalized weight of each of the fractions. This allows the validation of the SEC measurements by means of results obtained from fractional precipitation. However, it proves that the fractionation yield of 98.5% is sufficient to explain the small difference observed between the SEC chromatogram of the whole polymer and that reconstructed using the individual fractions.

SEC Autocalibration Procedure

The iterative procedure originally proposed by Purdon and Mate[46] for calibration with broad molecular weight distribution standards was used to calibrate the SEC columns with the same fractions characterized by light scattering. As seen in Figure 3, in the plot of log $\bar{M}_w$ versus t_e(peak) only a small type of deviation from linearity is observed, shown by the open circles. In SEC a polynomial is used to fit the calibration curve. In its general form the logarithm of the molecular weight and the elution time or volume are selected as function and variable, respectively. McCrackin[26] described a procedure that takes into account nonlinear effects by using a quadratic curve; Szewczyk[47–51] proposed an iterative

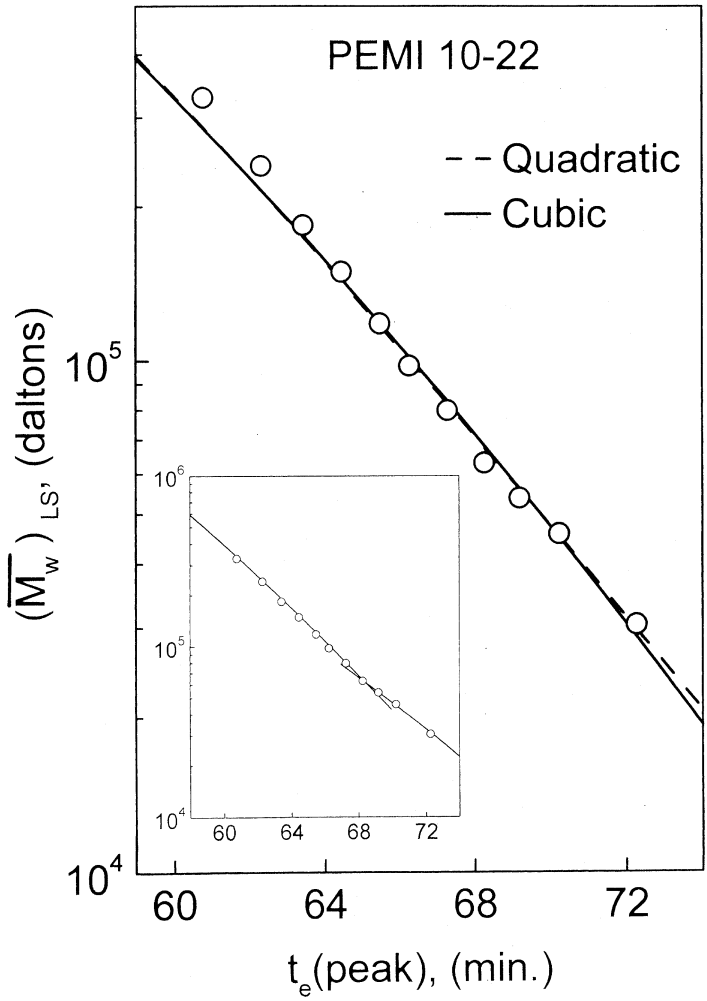

FIGURE 3 SEC calibration curves obtained for PEMI 10-22 fractions: open circles correspond to the experimental results, as a semilogarithm plot of the weight-average molecular weight $\log(\bar{M}_w)_{LS}$ of a series of fractions, against the elution time at the peak t_e(peak); the dotted line corresponds to the calibration curve fitted to the experimental results using a second-degree polynomial; the solid line corresponds to the calibration curve fitted to the experimental results using a third-degree polynomial.

method that can be applied to any polynomial of degree n. From a practical point of view this method was used[3] for another comb-like polymer, poly(*N*-[*n*-octadecyl]maleimide) (PMI 18). This method was based on the inversion of the calibration function $\log \bar{M}_w = f(t_e[\text{peak}])$ for the precise determination of the elution time $t_e(\text{peak}) = f^{-1}(\log \bar{M}_w)$. For this reason, a calibration function $M(t_e)$ of the polynomial type was assumed

$$\text{Log } M = \sum_{k=0}^{n} A_k t^k = A_0 + A_1 t_e + A_2 t_e^2 + A_3 t_e^3 + \cdots + A_n t_e^n \qquad (5)$$

where A_0, A_1, $A_2, \ldots A_n$ are the coefficients of the n-th order polynomial. Preliminary starting values for the coefficients A_0, A_1, $A_2, \ldots A_n$ were taken from results of $\log \bar{M}_w$ versus t_e(peak), where t_e(peak) is the peak elution time for the fractions measured by light scattering. With this initial correlation the weight-average molecular weight $(\bar{M}_w)_{cal}$ was calculated from the normalized chromatograms $H(t_e)_i$ for each one of the fractions, taking into account that

$$(\bar{M}_w)_{cal_i} = \int H(t_e)_i M(t_e) dt \qquad (6)$$

where $M(t_e)$ can be obtained by means of $10^{\log M}$. With the estimated values of $(\bar{M}_w)cal_i$ a new calibration function $M(t_e)$ can be calculated. In this way, the coefficients A_0, A_1, etc., can be optimized by means of an iterative process in which the function

$$s = \sum [(\bar{M}_{w_i}) - (\bar{M}_w)_{cal_i}]^2 \qquad (7)$$

is minimized by means of the nonlinear algorithm of Cholesky [52].

For this calculation process a package written in FORTRAN was developed whose results for a quadratic and a cubic polynomial function, respectively, are shown in Table II. The results of convergence for both approximations are plotted in Figure 4. It can be observed that, in both cases, the process is convergent with only a few iterations. It also can be observed that in both cases the sum of the squared deviations(s) is very small. It is reduced asymptotically as the order of the polynomial is increased, as shown in Figure 4. We have plotted in Figure 3 as dotted and full lines, the results for the quadratic and cubic functions, respectively, in a semilogarithm plot as well as weight-average molecular weight $\bar{M}_w$ measured by light scattering as a function of the elution time at the peak t_e(peak). Good agreement between the weight-average molecular weight $\bar{M}_w$ measured and calculated was obtained, as can be seen from Table III. Only a slight difference between the results from the quadratic and cubic functions was observed. However, they differ considerably

TABLE II Autocalibration results. Coefficients in Equation (5) defining the best calibration curve

	Polynomial degree	
	Quadratic	Cubic
Number of iterations	9	17
s	1021	768
A_0	8.72	15.31
A_1	-2.68×10^{-2}	-3.50×10^{-1}
A_2	-4.42×10^{-4}	4.82×10^{-3}
A_3		-2.84×10^{-5}

from the function obtained by means of the values of $(\bar{M}_w)_{LS}$, which represents only a first-order approximation. A cubic function was selected for calibration due to its simplicity and by the fact that an increase of the number of coefficients or degree of the polynomial does not produce any significant improvement in the accuracy of the results.

From the aforementioned calibration curve, it was possible to calculate molecular weight averages $\bar{M}_n$, $\bar{M}_w$, and $\bar{M}_z$ together with the polydispersity factor h for each fraction. The following relationships for the different molecular weight averages were used, where $H(t_e)_i$ is the normalized chromatogram. The number-average molecular weight $\bar{M}_n$ is given by

$$\bar{M}_n = \left\{ \int [1/M(t_e)] \cdot H(t_e) dt \right\}^{-1} \tag{8}$$

To obtain the weight-average molecular weight $\bar{M}_w$, Equation (6) was used. The z-average molecular weight $\bar{M}_z$ given by

$$\begin{aligned} \bar{M}_z &= \int H(t_e) M(t_e)^2 dt \Big/ \int H(t_e) M(t_e) dt \\ &= (1/\bar{M}_w) \int H(t_e) M(t_e)^2 dt \end{aligned} \tag{9}$$

and, finally, the polydispersity factor h can be expressed by $h = \bar{M}_w/\bar{M}_n$.

At this stage, the viscosity-average molecular weight $\bar{M}_v$ can be estimated. However this was not carried out because the viscometric results obtained for the polymer fractions did not produce a unique pair of values for the parameters in the Mark-Houwink equation. Two well-differentiated trends were obtained when the intrinsic viscosity $[\eta]$ was plotted against the molecular weight M on a log-log scale. The first trend corresponded to the low molecular weight region, where for a given value

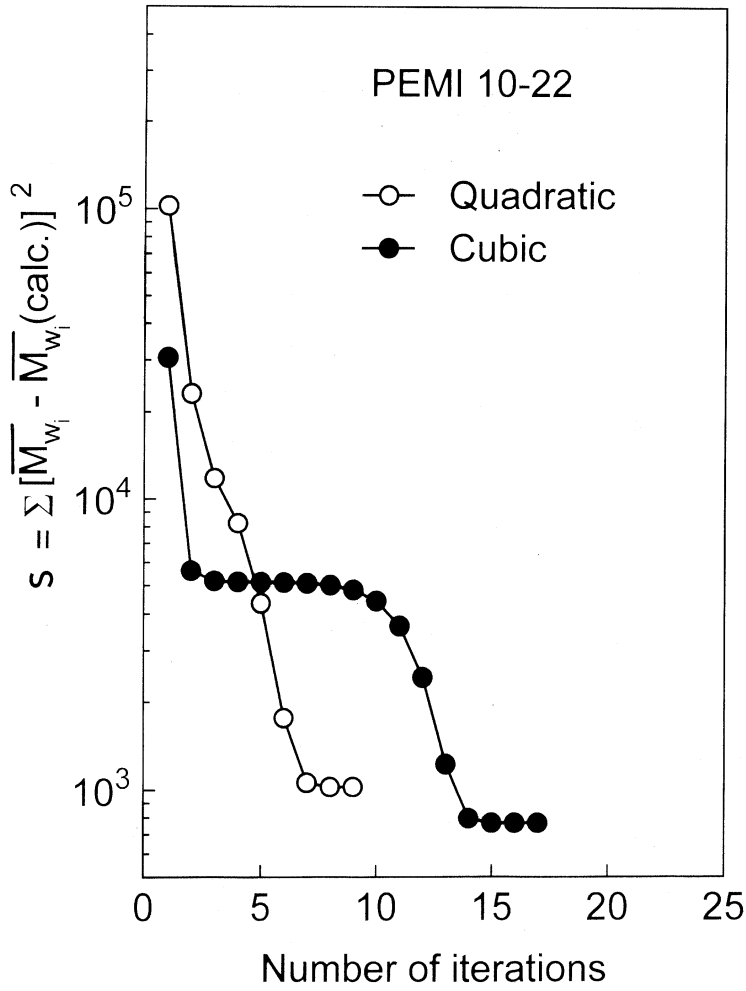

FIGURE 4 Plot of σ, sum of the squared deviations, as a function of the number of iterations for the quadratic function and cubic function approximations. The calibrating equation is a polynomial of the form $\log M = A_0 + A_1 t_e + A_2 t_e^2 + \cdots + A_n t_e^n$ and the fitting procedure is an iterative one as explained in a previous section.

of the molecular weight M the intrinsic viscosity $[\eta]$ was found to be almost independent of molecular weight. However, in the high molecular weight region, the Mark–Houwink equation was obeyed[37]. It should be noted that it was necessary to measure the crossover point very precisely

TABLE III Size exclusion chromatography data of poly(*N*-[10-(*n*-docosane[oxycarbonyl])-*n*-decyl maleimide]) PEMI 10–22, elution time at the peak t_e(peak), weight-average molecular weight measured by light scattering $(\bar{M}_w)_{LS}$, weight-average molecular weight $(\bar{M}_w)_{SEC}$, number-average molecular weight $(\bar{M}_n)_{SEC}$, and polydispersity factor $h = (\bar{M}_w)_{SEC}/(\bar{M}_n)_{SEC}$

Fraction number	t_e(peak) (min)	$(\bar{M}_w)_{LS}$ $\times 10^{-3}$	$(\bar{M}_w)_{SEC}$ $\times 10^{-3}$	$(\bar{M}_n)_{SEC}$ $\times 10^{-3}$	$h = (\bar{M}_w)_{SEC}/(\bar{M}_n)_{SEC}$
F-1	60.8	329.0	328.9	139.2	2.36
F-2	62.3	241.0	241.5	130.5	1.85
F-3	62.6		201.0	110.5	1.82
F-4	63.4	184.0	183.8	110.8	1.66
F-5	63.7		163.3	110.6	1.48
F-6	64.5	149.0	148.3	106.0	1.40
F-7	64.8		133.0	92.8	1.43
F-8	65.5	118.2	116.7	85.3	1.37
F-9	65.8		108.2	77.7	1.39
F-10	66.3	97.8	97.9	71.8	1.37
F-11	67.1		82.5	61.6	1.34
F-12	67.3	79.9	79.1	60.7	1.30
F-13	67.8		69.9	55.9	1.25
F-14	68.3	63.0	64.1	48.0	1.34
F-15	69.2	53.7	54.7	43.0	1.27
F-16	70.2	45.7	45.4	36.6	1.24
F-17	71.3		35.9	27.6	1.30
F-18	72.3	30.4	29.9	24.5	1.22
F-19	74.0		20.7	16.8	1.23
F-20	76.0		12.8	9.8	1.30

in order to carry out the numerical integration of the chromatograms. Values of $\bar{M}_v$ and how they are estimated will be given in a forthcoming paper[37]. This effect can be easily observed in the magnified region shown in Figure 3. The calibration curve is in fact composed of two curves, one for the high molecular weight and the other for the lower molecular weight species. However, this behavior does not appreciably affect the values of the number-weight and z-averages calculated using the cubic polynomial. This can be attributed to the minimal difference in slopes of the two curves' increase. Therefore, the slight increase in precision does not justify the complexity in subsequent calculations if two regimes in the calibration curve are considered. Nevertheless, the viscosity-average molecular weight $\bar{M}_v$ needs to be calculated considering this effect, and two series of values of the two Mark–Houwink equations were also needed in order to describe this apparent peculiar behavior, which

indicates the presence of other linear and branched macromolecules, as will be explained later in more detail[37].

The above calculations were performed by means of a program written in FORTRAN, using the method of Simpson for numerical integration, and its simplicity and validity were considered. The estimated values are shown in Table III and are plotted as a semilogarithm function against the peak chromatogram elution time t_e(peak) in Figure 5. In all cases a smooth variation is apparent between data. In Figure 6 we have plotted the polydispersity factor of the fractions as a function of the peak elution time t_e(peak). It was found to decrease gradually, as expected.

Simulated Fractionation from Fractional Precipitation Data

Even though the solubility of polymer molecules can be explained qualitatively in terms of the Flory–Huggins theory, there has traditionally existed an enormous quantitative gap between the simplified theory of phase equilibrium and the experimental conditions employed in fractionation. Tung[53] was the first to develop a computational simulation of the SPF (successive precipitation fractionation) method by taking into account the theory of Flory-Huggins. Subsequently, Kamide et al.[6,9,12,54–72] and Koningsveld and Staverman[10,11] developed this computational method to investigate the effect of the different variables that influence this process. However, as far as the present authors are aware no comparison between the results of these types of calculations and those obtained experimentally has been attempted.

In this study, due to the accurate fractional precipitation data obtained for a large number of fractions and their characterization, further complemented by detailed SEC information, a simulation and comparison between the results and experimental data is attempted.

It is necessary to note that the algorithm employed in the calculations corresponds to the SPF method (successive precipitation fractionation), which is a different experimental technique. That is, the separation of phases by diminishing the temperature of the whole system has been replaced by the addition of a precipitant at a constant temperature (isothermal). However, when applied, the results obtained are, as mentioned previously, equivalent. Therefore, the use of computational operations in order to calculate the distributions and molecular parameters measured experimentally was attempted.

Theory of Phase Separation

According to the theory of Flory-Huggins, the chemical potential of dilution of the solvent, $\Delta\mu_0$, and a polymer of polymerization degree X,

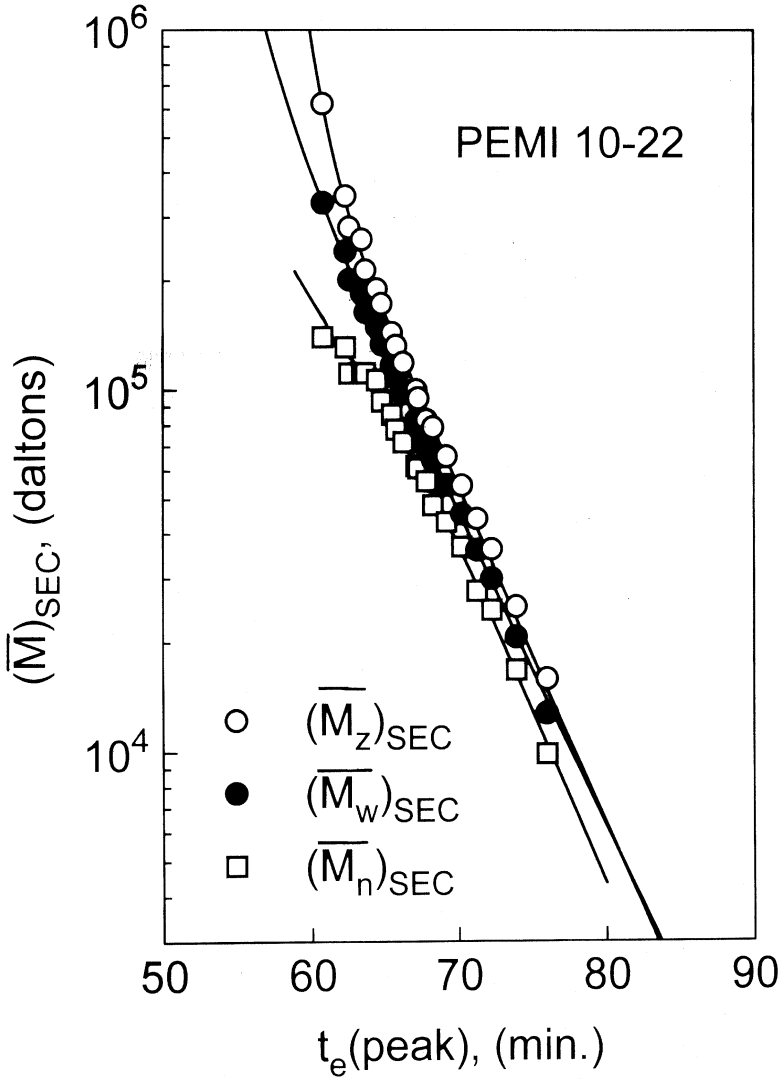

FIGURE 5 Molecular weight averages estimated from SEC data using an autocalibration method as a function of the elution time t_e(peak).

$\Delta\mu_x$, in a solution is given by means of the following expressions, respectively:

$$\Delta\mu_0 = RT\{\ln(1 - v_p) + [1 - (1/\bar{X}_n)]v_p + \chi v_p^2\} \tag{10}$$

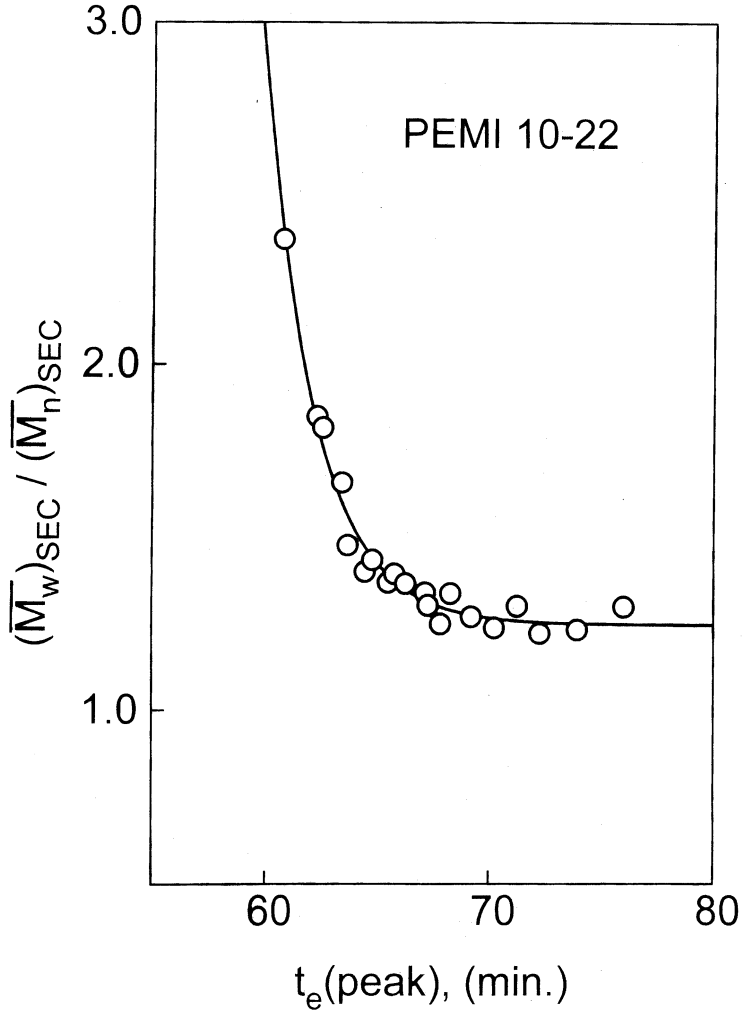

FIGURE 6 Polydispersity factor estimated from SEC data and autocalibration method $(\bar{M}_w)_{SEC}/(\bar{M}_n)_{SEC}$ for a series of fractions of poly(*N*-[10-(*n*-docosane[oxycarbonyl])-*n*-decyl maleimide]) PEMI 10-22 as a function of the elution time. The circles correspond to the values obtained using a third-degree polynomial.

$$\Delta\mu_x = RT\{\ln v_x - (X-1) + X[1-(1/\bar{X}_n)]v_p + \chi X(1-v_p)^2\} \qquad (11)$$

where R is the gas constant, T is the absolute temperature, v_p is the polymer concentration expressed as the volume molar fraction of the polymer, and $\bar{X}_n$ is the number-average degree of polymerization.

The polymer/solvent interaction parameter χ in Equation (10), according to the theory of Flory-Huggins, is a function of the temperature and is independent of the concentration. However, experimentally it has been found that χ depends on concentration. This dependence can be expressed by means of the following expression:

$$\chi = \chi_0(1 + pv_p) \qquad (12)$$

where χ_0 is a constant and p is a characteristic parameter to express the concentration dependence of χ. The validity of Equation (12) has been shown for various polymer solutions [73]. Taking this dependence into account, Equation (10) can be rewritten as follows:

$$\Delta\mu_0 = RT\{\ln(1-v_p) + [1-(1/\bar{X}_n)]v_p + \chi_0(1+pv_p)\,v_p{}^2\} \qquad (13)$$

When χ can be expressed by Equation (12), Equation (11) can be derived directly[7] or by means of a series of arguments[60] as follows:

$$\Delta\mu_x = RT\{\ln v_x - (X-1) + X[1-(1/\bar{X}_n)]v_p + \chi_0 X(1-v_p)^2 + \chi_0 pX(0.5 - 1.5\,v_p{}^2 + v_p{}^3)\} \qquad (14)$$

When the equilibrium between the two liquid phases is reached, i.e., they are in thermodynamic equilibrium, the following holds:

$$\Delta\mu_{0(1)} = \Delta\mu_{0(2)} \qquad (15)$$

$$\Delta\mu_{x(1)} = \Delta\mu_{x(2)} \qquad (16)$$

where subscripts 1 and 2 represent the diluted (supernatant) polymer phase and the concentrated (precipitate) polymer phase, respectively. The substitution of $\Delta\mu_0$ in Equation (13) into Equation (15) yields:

$$\chi_0 = \{1/[(v_{p(2)}{}^2 - v_{p(1)}{}^2) + p(v_{p(2)}{}^3 - v_{p(1)}{}^3)]\} \cdot \{\ln[(1-v_{p(1)})/(1-v_{p(2)})] + [1-(1/\bar{X}_{n_{(1)}})]v_{p(1)} - [1-(1/\bar{X}_{n_{(2)}})]v_{p(2)}\} \qquad (17)$$

The combination of Equations (14) and (16) gives:

$$\ln v_{x(2)} - \ln v_{x(1)} = \sigma X \qquad (18)$$

where

$$\sigma = [1 - (1/\bar{X}_{n_{(1)}})]v_{p(1)} - [1 - (1/\bar{X}_{n_{(2)}})]v_{p(2)} - \chi_0[2(v_{p(2)} - v_{p(1)}) + v_{p(1)}^2 - v_{p(2)}^2] + \chi_0 p[v_{p(1)}^3 - v_{p(2)}^3 - 1.5(v_{p(1)}^2 - v_{p(2)}^2)] \quad (19)$$

Eliminating χ_0 between Equations (17) and (19), the following is obtained:

$$\sigma = \{[2 + 1.5p(v_{p(2)} + v_{p(1)})]/[(v_{p(2)} + v_{p(1)}) + p(v_{p(2)}^2 + v_{p(2)}v_{p(1)} + v_{p(1)}^2)]\} \cdot \{\ln[(1 - v_{p(1)})/(1 - v_{p(2)})] + [1 - (1/(\bar{X}_{n_{(1)}})]\, v_{p(1)} - [1 - (1/\bar{X}_{n_{(23)}})]\, v_{p(2)}\} - \ln[(1 - v_{p(1)})/(1 - v_{p(2)})] \quad (20)$$

However, if the volume ratio R, defined by

$$R = V_{(1)} / V_{(2)} \quad (21)$$

where $V_{(i)}$ is the volume of the respective phase and V the total volume of both phases ($V = V_{(1)} + V_{(2)}$), they are expressed as follows:

$$V_{(1)} = RV/(R + 1) \quad (22)$$

$$V_{(2)} = V/(R + 1) \quad (23)$$

If the fraction of a given *X-mer* remaining in both phases is designated by $f_{x(1)}$ and $f_{x(2)}$, respectively, the corresponding weights are given by

$$g_{(2)}(X) = f_{x(2)}\, g_0(X) = g_0(X) \exp(\sigma X)/[R + \exp(\sigma X)] \quad (24)$$

$$g_{(1)}(X) = f_{x(1)}\, g_0(X) = R\, g_0(X)/[R + \exp(\sigma X)] \quad (25)$$

where $g_0(X)$ represents the weight of the *X-mer* dissolved in the original mother solution.

Equations (24) and (25) were obtained from Equation (18) under the assumption that the specific volumes of the macromolecules are constant (1.00) and independent of the degree of polymerization.

Using Equations (22) and (23) the concentrations of the polymer in both phases are given by

$$v_{p(1)} = (1/V_{(1)}) \cdot \sum g_{(1)}(X) = [(1 + R)/VR] \cdot \sum g_{(1)}(X) \quad (26)$$

$$v_{p(2)} = (1/V_{(2)}) \cdot \sum g_{(2)}(X) = [(1 + R)/V] \cdot \sum g_{(2)}(X) \quad (27)$$

Finally, the number-average molecular weights of the polymer in both phases can be calculated by means of the following expressions:

$$\bar{X}_{n(1)} = \sum g_{(1)}(X) / \sum (1/X) g_{(1)}(X) \tag{28}$$

$$\bar{X}_{n(2)} = \sum g_{(2)}(X) / \sum (1/X)\, g_{(2)}(X) \tag{29}$$

obtained from Equations (28) and (29).

This theoretical approach was developed for experimental results of fractionations obtained by successive precipitation fractionation (SPF) or by successive solutional fractionation (SSF). In both cases the original polymer sample is dissolved in a single solvent, to give V_0 mL of solution. In SPF, on lowering the temperature of the solution stepwise, the precipitates are successively separated from the solution. The original volume V_0 is practically maintained throughout the fractionation. On the contrary, in SSF, on lowering the solution temperature, the polymer-lean phase is separated from the solution. The fraction is isolated from this phase using a standard procedure. Further solvent is added to the polymer-rich phase to maintain the solution with V_0 mL, and the temperature lowered again and the process repeated. Therefore, in both cases the V_0 does not change during the course of separation. This is the fundamental assumption when the above equations are applied. In the experimental procedure used in this study, i.e., fractional precipitation, this condition is not fulfilled.

Procedure of Computational Simulation

The computational simulation of the fractionation was carried out by means of a FORTRAN package program using the above equations. The following scheme of calculation was applied:

It was assumed one gram of unfractionated sample, $\Sigma g_o(X) = 1$, of the polymer dissolved in a volume V_0 of solvent would give a concentration equal to that of the original mother solution of the whole polymer. The weight-average molecular weight distribution $g_0(X)$ of the whole polymer, namely, the unfractionated polymer, is obtained from the SEC chromatogram $H(t_e)$, shown by the continuous line in Figure 1. These are related by means of the following expression:

$$g(X) = -H(t_e)dX/dt = -H(t_e)/2.303\ sX \tag{30}$$

where $s = d(\log X)/dt$ is obtained from the slope of the calibration curve given in Figure 3. For each fraction the starting weight was taken as the weight of the fraction $\Sigma g_2(X)$, obtained experimentally. These weights are shown in Table I. The following steps were followed:

(1) Arbitrary values were assigned to R and $\bar{X}_{n(2)}$.
(2) By means of Equations (22) and (23) $V_{(1)}$ and $V_{(2)}$ were calculated.
(3) From the values obtained that of $\Sigma g_1(X) = 1 - \Sigma g_2(X)$, $v_{p(1)}$ and $v_{p(2)}$ were calculated by means of Equations (26) and (27), respectively.
(4) The estimation of σ was obtained using Equation (20) and values obtained.
(5) At this point, sufficient data has been calculated to calculate the molecular weight distributions $g_i(X)$, according to Equations (24) and (25), respectively.
(6) The calculation of the weights, $\Sigma g_i(X)$, and the average molecular weights $\bar{X}_{n(i)}$, using Equations (28) and (29), were employed as criteria of convergence when compared with the values taken initially in step (1). These values were corrected by means of the estimated values followed by further iteration and was reinitiated until the convergence between both values lay within 2%.

The data for the successive fractions were calculated employing the same procedure but then replacing the values of $g_0(X)$ and V_0 of the first fraction by the molecular weight distribution curve of the polymer and the volume that the new diluted phase obtained in the previous step but ignoring the addition of new volume of the precipitant agent.

The last fraction was obtained by a hypothetical evaporation of the solvent of the aforementioned supernatant phase calculated in the last iteration.

The parameter p, defined in Equation (12), was assumed to be constant throughout the fractionation. In this study the value of p was taken as 0.77. This value was estimated by adjusting the values of $\bar{X}_n$ and $\bar{X}_w$ calculated for the first two fractions with their respective experimental values, i.e., a parameter that can be adjusted using the experimental results for the two first fractions obtained from fractionation.

DISCUSSION OF RESULTS

The results obtained by applying the method outlined in the previous section are shown in Table IV. The validity of this method can be seen in Figures 7 and 8, where the averages $\bar{M}_n$ and $\bar{M}_w$ and corresponding polydispersity factor $h = \bar{M}_w/\bar{M}_n$, obtained experimentally, are compared with those obtained by computational simulation. Good agreement is observed between the molecular weight averages and the polydispersity factor h. Therefore the assumption of a constant value for the parameter p during the course of fractionation is a valid hypothesis. Figure 7 also shows that there is good agreement between the values of $\bar{M}_w$ and $\bar{M}_n$ for all fractions.

In Figures 9 and 10 two important factors that control the phase separation phenomena, i.e., the concentration of the polymer-rich phase

TABLE IV Fractional precipitation data from simulation of poly(*N*-[10-(*n*-docosane[oxycarbonyl])-*n*-decyl maleimide]) PEMI 10-22, volume of precipitate $V_{(2)}$, number-average molecular weight $(\bar{M}_n)_{sim}$, weight-average molecular weight $(\bar{M}_w)_{sim}$, polydispersity factor $h_{sim} = (\bar{M}_w)_{sim}/(\bar{M}_n)_{sim}$, polymer concentration V_p, volume ratio R, and partition coefficient σ

Fraction number	$V_{(2)}$ (mL)	$(\bar{M}_w)_{sim}$ $\times 10^{-3}$	$(\bar{M}_n)_{sim}$ $\times 10^{-3}$	$h_{sim} = (\bar{M}_w)_{sim}/(\bar{M}_n)_{sim}$	V_p (g·mL^{-1})	R	σ $\times 10^5$
F-1	0.30	321.4	127.9	2.51	0.119	193	1.08
F-2	0.52	248.7	115.7	2.15	0.121	111	1.35
F-3	0.39	207.8	106.6	1.95	0.122	146	1.56
F-4	0.33	184.2	101.0	1.82	0.123	173	1.75
F-5	0.41	163.5	95.0	1.72	0.124	138	1.99
F-6	0.54	142.8	87.8	1.63	0.125	103	2.33
F-7	0.33	129.7	83.1	1.56	0.126	165	2.60
F-8	0.43	116.6	77.8	1.50	0.128	129	2.99
F-9	0.42	104.6	72.2	1.45	0.129	130	3.43
F-10	0.43	93.2	66.3	1.41	0.131	127	3.96
F-11	0.36	83.7	61.5	1.36	0.133	147	4.64
F-12	0.26	76.0	57.2	1.33	0.134	206	5.22
F-13	0.30	68.2	52.6	1.30	0.136	179	6.05
F-14	0.32	59.9	47.2	1.27	0.138	162	7.18
F-15	0.31	51.8	41.9	1.24	0.141	168	8.76
F-16	0.40	42.3	35.0	1.21	0.146	129	11.5
F-17	0.28	34.3	29.3	1.17	0.151	187	15.1
F-18	0.27	27.1	23.7	1.15	0.157	188	20.5
F-19	0.31	19.9	17.6	1.13	0.169	165	32.2
F-20	0.24	12.6	11.2	1.13	0.195	213	66.8

v_p and the volume ratio R, are plotted against fractionation order (fraction number).

Due to the good agreement obtained for the molecular parameters (molecular averages and distributions), this method of simulation fractionation corresponds to the equivalent thermal successive precipitation fractionation (SPF). That is, even though the equilibrium conditions may be equivalent, the operating conditions are not. This may be why the value of the extensive magnitudes (concentration, volume ratio) depicted in Figures 9 and 10 follow the same tendency but were not predicted correctly using this model. Nevertheless, the partition coefficient σ shown in Figure 11, which is also an intensive magnitude, follows the usual exponential dependence.

The difference between methods can be attributed to differences in the experimental procedures. That is, fractionation is based in the successive

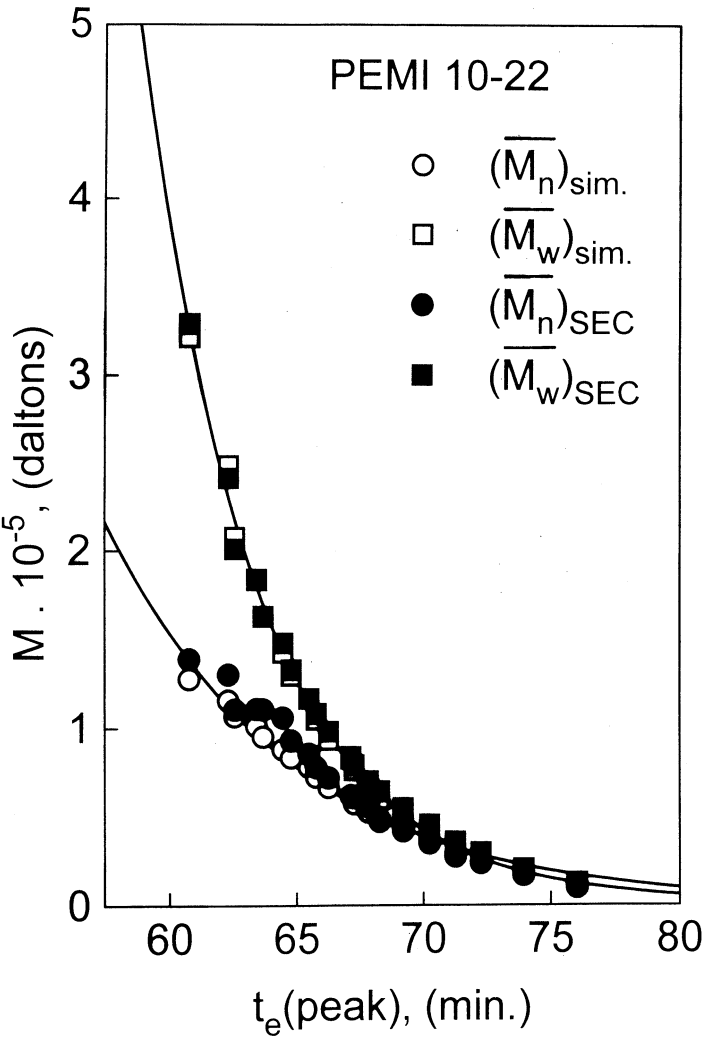

FIGURE 7 Comparison of the molecular weight averages estimated by the autocalibration method from SEC data and those obtained using a simulation method and experimental data from fractional precipitation.

addition of known volumes of precipitant, whereas in the simulation procedure, successive precipitation fractionation (SPF), the fractions are not produced by the addition of precipitant but by decreasing the temperature of the system.

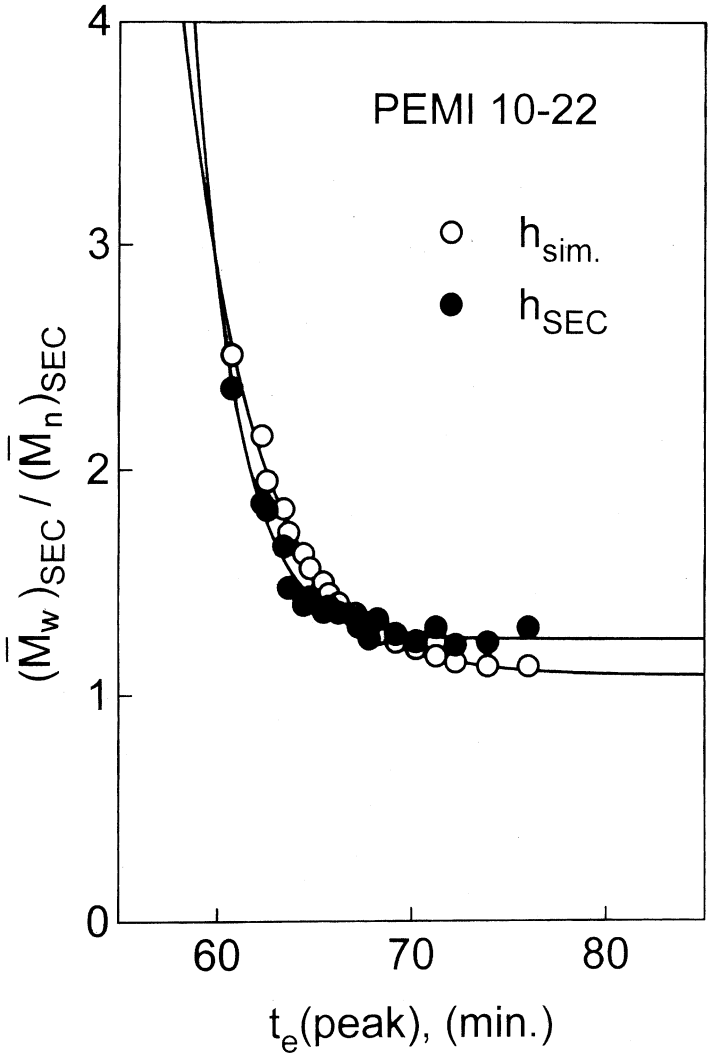

FIGURE 8 Comparison of experimental and simulated polydispersity factor $h = \bar{M}_w/\bar{M}_n$ as a function of elution time of the fractions.

Figure 12, however, shows the weight-average molecular weight distributions for a series of fractions and the whole polymer. These distribution were also obtained by simulation and clearly show how the

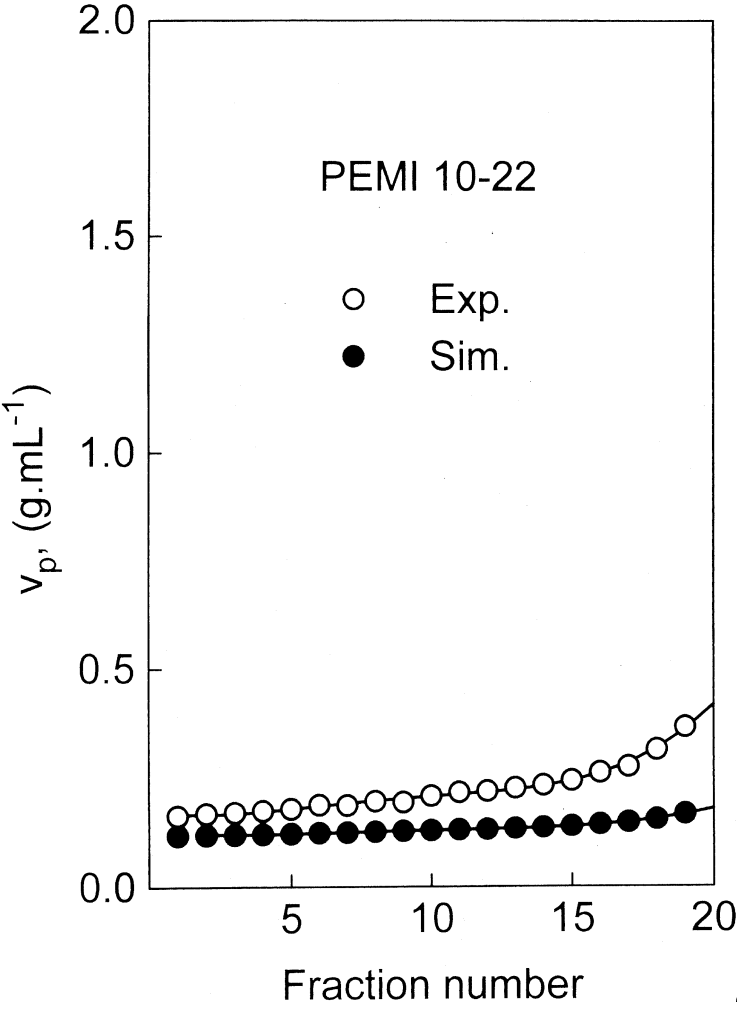

FIGURE 9 Dependence of the experimental and simulated concentration of the polymer-rich phase against the fractionation order for a series of fractions of poly(*N*-[10-(*n*-docosane[oxycarbonyl])-*n*-decyl maleimide]) PEMI 10-22.

width of the distribution is drastically reduced as the fractionation increases. As seen in Figure 12, successive fractions tend towards a normal Gaussian distribution. In fact, this is quite normal because successively the mother solution has a more normalized molecular weight

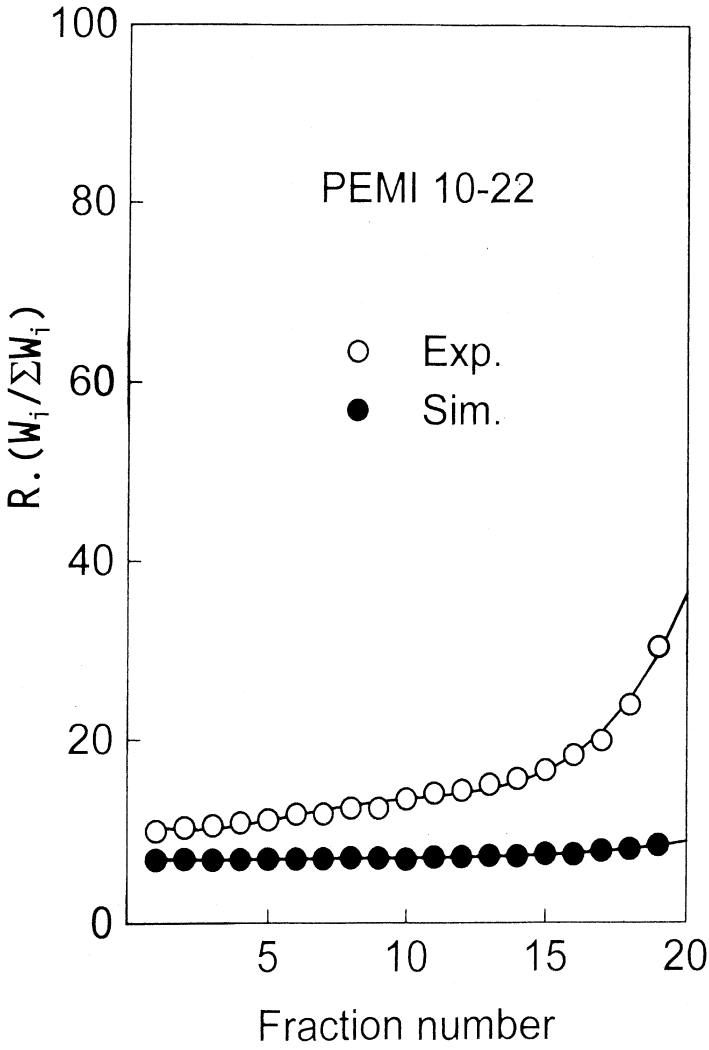

FIGURE 10 Dependence of the experimental and simulated weight normalized volume ratio $R.(W_i/\Sigma W_i)$ against the fractionation order (fraction number) for a series of fractions of poly(*N*-[10-(*n*-docosane[oxycarbonyl])-*n*-decyl maleimide]) PEMI 10-22.

distribution. Therefore, it can be proposed that the fractionation of polymers is equivalent to a deconvolution of a normally complex mother distribution into normal Gaussian fractions.

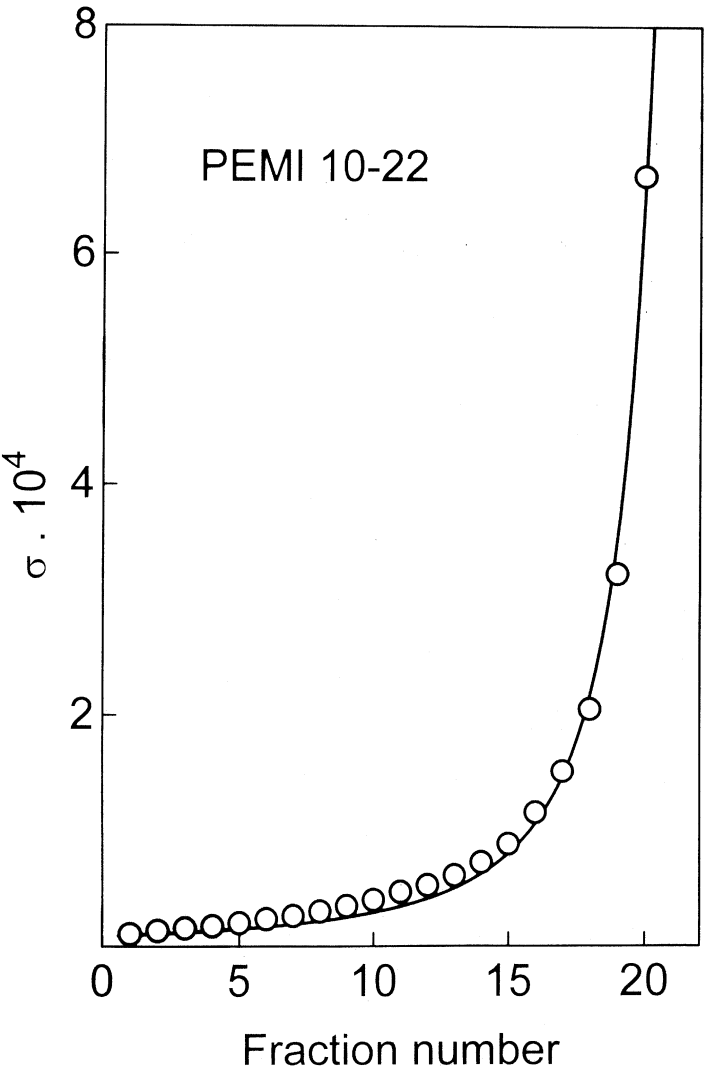

FIGURE 11 Plot of the partition coefficient *s* against fractionation order for poly(*N*-[10-(*n*-docosane[oxycarbonyl])-*n*-decyl maleimide]) PEMI 10-22.

CONCLUSIONS

To avoid the use of a universal calibration procedure, a modified method has been described and used to prepare a calibration curve

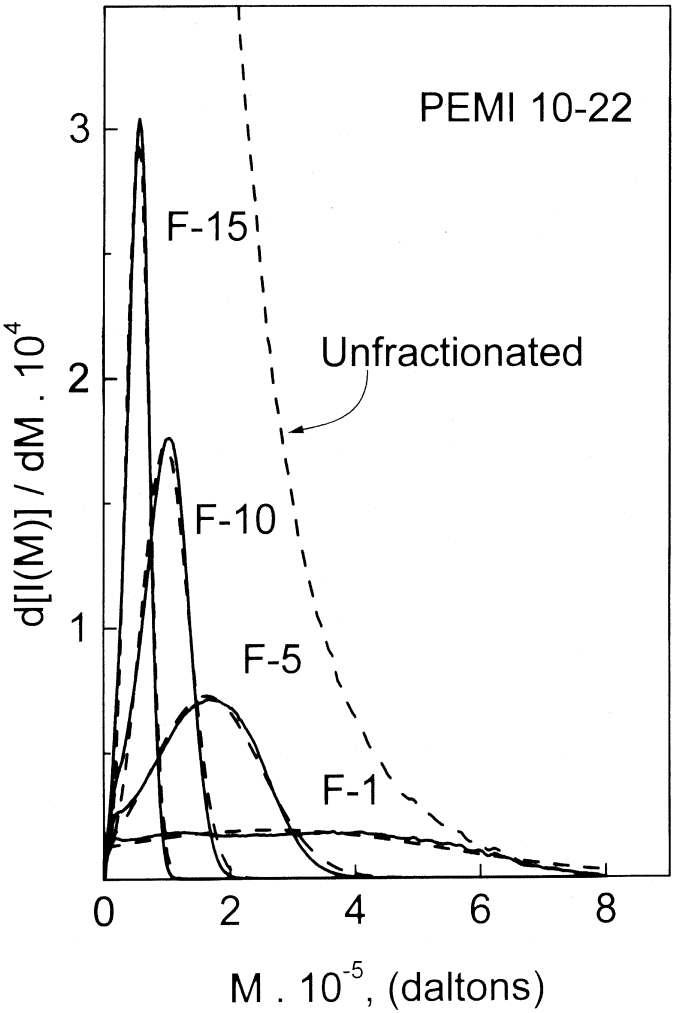

FIGURE 12 Molecular weight differential distribution $g(X) \equiv d[I(M)]/dM$ for a series of fractions and the unfractionated polymer, calculated using a simulation method and experimental data from fractional precipitation for poly(*N*-[10-(*n*-docosane[oxycarbonyl])-*n*-decyl maleimide]) PEMI 10-22. Dotted lines represent the fitted Gaussian distributions.

for the polymer fractions. From these results it can be concluded that the method of autocalibration may be useful only when a number of fractions of the polymer over a wide molecular weight distribution is

available. The technique offers the advantage that it requires only data from the SEC chromatograms and one average of the molecular weight of some of the fractions. The method may also be very useful in cases where non-exclusion SEC effects occur during the elution process.

The simulation procedure proposed by Kamide et al.[9,54–56] and improved by Kamide and Sugamiya[59] based on the Flory-Huggins solution theory, and fractionation data obtained from successive precipitation fractionation (SPF) or successive solutional fractionation (SSF), were applied and tested on fractions obtained by isothermal fractional precipitation. In this case it is necessary to know in advance the initial concentration or the polymer volume fraction in the solution $v^0{}_p$ as well as the relative amount or size of each fraction ρ, besides the values of X_n of the two first fractions, to adjust the parameter p. Furthermore, the experimental molecular weight data for fractions demonstrate excellent agreement when compared with results obtained by several independent measurements, such as fractional precipitation, light scattering, and size exclusion chromatography. These results further suggest that both the methods of calibration and simulation are readily applicable to cases where only broad molecular weight fractions are available.

In general, fractionation is a preparative method to obtain polymer fractions for subsequent characterization. However, it may also be used as a procedure to obtain standard fractions of known molecular weight distribution for analysis by SEC or SEC autocalibration, the results of which would facilitate the analysis of theories on phase separation.

Finally, the apparent validity of the molecular parameters obtained by simulation show the usefulness of this technique. That is, this calculation requires knowledge only of the initial molecular weight distribution and the weight fraction, which in turn decreases the workload necessary to determine the data analytically (i.e., SEC, light scattering).

REFERENCES

[1] Tung, L. H. (1971). *J. Macromol. Sci.-Revs. Macromol. Chem.*, **C6**, 51.

[2] Barrales-Rienda, J. M., Bello, A., Bello, P., and Guzmán, G. M. (1999). Fractionation of Polymers, in *Polymer Handbook*. 4th ed., J. Brandrup, E. H. Immergut, and E. A. Grulke, eds., John Wiley, New York.

[3] Barrales-Rienda, J. M., Romero Galicia, C., and Horta, A. (1983). *Macromolecules*, **16**, 932.

[4] Kotera, A. (1967). Fractional Precipitation, in *Polymer Fractionation*, M. J. R. Cantow, ed., Academic Press, New York, ch. B.1.

[5] Elliot, J. H. (1967). Fractional Solution, in *Polymer Fractionation*, M. J. R. Cantow, ed., Academic Press, New York ch. B.2.

[6] Kamide, K. (1977). Batch Fractionation, in *Fractionation of Synthetic Polymers: Principles and Practices*. L. H. Tung, ed., Marcel Dekker, New York, ch. 2.

[7] Huggins, M. L. and Okamoto, H. (1967). Theoretical Considerations, in *Polymer Fractionation*, M. J. R. Cantow, ed., Academic Press, New York, ch. A.
[8] Huggins, M. L. (1967). *J. Polym. Sci., Part A-2*, **5**, 1221.
[9] Kamide, K., Ogawa, T., Sanada, M., and Matsumoto, M. (1968). *Kobunshi Kagaku (Chem. High Polymers)*, **25**, 440.
[10] Koningsveld, R. and Staverman, A. J. (1968). *J. Polym. Sci. A-2*, **6**, 367.
[11] Koningsveld, R. and Staverman, A. J. (1969). *J. Polym. Sci. A-2*, **6**, 383.
[12] Kamide, K. (1974). *Kobunshi Ronbunshu*, **31**, 147.
[13] Barth, H. G., Boyes, B. E., and Jackson, C. (1996). *Anal. Chem.*, **68**, 445R.
[14] Barth, H. G., Boyes, B. E., and Jackson, C. (1998). *Anal. Chem.*, **70**, 251R.
[15] Jackson, C. and Barth, H. G. (1995). In *Chromatographic Characterization of Polymers. Hyphenated and Multidimensional Techniques*, T. Provder, H. G. Barth, and M. W. Urban, ed., Advances in Chemistry Series 247, American Chemical Society, Washington, DC, 59–68.
[16] Jackson, C. and Barth, H. G. (1994). *Trends Polym. Sci.*, **2**, 203.
[17] Jackson, C. and Barth, H. G. (1995). In *Molecular Weight Sensitive Detectors for Size Exclusion Chromatography*, C. S. Wu, ed., Marcel Dekker, New York, ch. 4, 103–145.
[18] Barth, H. G. (1994). In *Hyphenated Techniques in Polymer Characterization*, T. Provder, M. W. Urban, and H. G. Barth, eds., ACS Symposium Series 581, American Chemical Society, Washington, DC, 3–11.
[19] Sheng, L.-S., Shew, S. L., Winger, B. E., and Campana, J. E. (1994). In *Hyphenated Techniques in Polymer Characterization*, T. Provder, M. W. Urban, and H. G. Barth, eds., ACS Symposium Series 581, American Chemical Society, Washington, DC, ch. 5, 55–72.
[20] Benoît, H. C. (1996). *J. Polym. Sci: Part B: Polym. Phys.*, **34**, 1703.
[21] Procházka, O. and Kratochvíl, P. (1986). *J. Appl. Polym. Sci.*, **31**, 919.
[22] Procházka, O. and Kratochvíl, P. (1987). *J. Appl. Polym. Sci.*, **34**, 2325.
[23] Balke, S. T., Hamielec, A. E., Leclair, B. P., and Pearce, S. L. (1969). *Ind. Eng. Chem. Prod. Res. Dev.*, **8**, 54.
[24] Loy, B. R. (1976). *J. Polym. Sci., Polym. Chem. Ed.*, **14**, 2321.
[25] Vrijbergen, R. R., Soeteman, A. A., and Smit, J. A. M. (1978). *J. Appl. Polym. Sci.*, **22**, 1267.
[26] McCrackin, F. L. (1977). *J. Appl. Polym. Sci.*, **21**, 191.
[27] Mahabadi, H. K. and O'Driscoll, K. F. (1977). *J. Appl. Polym. Sci.*, **21**, 1283.
[28] Mori, S. and Suzuki, T. (1980). *J. Liq. Chromatogr.*, **3**, 343.
[29] Weiss, A. R. and Cohn-Ginsberg, E. (1970). *J. Polym. Sci., A-2*, **8**, 148.
[30] Morris, M. C. (1971). *J. Chromatogr.*, **55**, 203.
[31] Hamielec, A. E. and Omorodin, S. N. E. (1980). *Am. Chem. Soc. Symp. Ser.*, **138**, 183.
[32] Mori, S. (1981). *Anal. Chem.*, **53**, 1813.
[33] Purdom, Jr., J. R. and Mate, R. D. (1967). *Rubber World*, **155**, 22.
[34] Harmon, D. J. (1965). *J. Polym. Sci. Part C, Polym. Symp.*, **8**, 243.
[35] Barrales-Rienda, J. M., Galera Gómez, P. A., Horta, A., and Sáiz, E. (1985). *Macromolecules*, **18**, 2572.
[36] Barth, H. G. (1987). In *Detection and Data Analysis in Size Exclusion Chromatography*, T. Provder, ed., ACS Symposium Series 352, American Chemical Society, Washington, DC, 29–46.
[37] Carazo Chico, E. and Barrales-Rienda, J. M. *Polymer*, submitted.

[38] Riddick, J. A. and Bunger, W. B. (1970). *Organic Solvents: Physical Properties and Methods of Purification*, Techniques of Chemistry, vol. II, 3rd ed., Wiley-Interscience, New York, 220.
[39] Barrall II, E. M., Cantow, M. J. R., and Johnson, J. F. (1968). *J. Appl. Polym. Sci.*, **12**, 1373.
[40] Wagner, H. L. and Hoeve, C. A. J. (1971). *J. Polym. Sci. A-2*, **9**, 1763.
[41] Rhein, R. A. and Lawson, D. D. (1971). *Chem. Technol.*, **1**, 122.
[42] Menin, J. P. and Roux, R. (1972). *J. Polym. Sci. A-1*, **10**, 855.
[43] Candau, F., Francois, J., and Benoît, H. (1974). *Polymer*, **15**, 626.
[44] Chance, R. R., Baniukiewicz, S. P., Mintz, D., Ver Strate, G., and Hadjichristidis, N. (1995). *Int. J. Polym. Anal. Charact.*, **1**, 3.
[45] McCrackin, F. L. and Wagner, H. L. (1980). *Macromolecules*, **13**, 685.
[46] Purdon, Jr., J. R. and Mate, R. D. (1968). *J. Polym. Sci. Polym. Chem. Ed.*, **6**, 243.
[47] Szewczyk, P. (1976). *Polymer*, **17**, 90.
[48] Szewczyk, P. (1980). *J. Polym. Sci. Part C*, **68**, 191.
[49] Szewczyk, P. (1986). *J. Liq. Chromatog.*, **9**, 1175.
[50] Szewczyk, P. (1981). *J. Appl. Polym. Sci.*, **26**, 2727.
[51] Szewczyk, P. (1986). *Polymery*, **31**, 8.
[52] Forsythe, G. and Moler, C. B. (1967). *Computer Solution of Linear Algebraic Systems*, Prentice-Hall, Englewood Cliffs, NJ Carnahan, B., Luther, H. A., and Wilkes, J. O. (1969). *Applied Numerical Methods*, John Wiley, New York.
[53] Tung, L. H. (1962). *J. Polym. Sci.*, **61**, 449.
[54] Kamide, K., Ogawa, T., and Matsumoto, M. (1968). *Kobunshi Kagaku (Chem. High Polymers)*, **25**, 788.
[55] Kamide, K. and Nakayama, C. (1969). *Makromol. Chem.*, **129**, 289.
[56] Kamide, K., Ogawa, T., and Nakayama, C. (1970). *Makromol. Chem.*, **132**, 65.
[57] Kamide, K. and Nakayama, C. (1970). *Makromol. Chem.*, **135**, 9.
[58] Kamide, K., Sugamiya, K., Ogawa, T., Nakayama, C., and Baba, N. (1970). *Makromol. Chem.*, **135**, 23.
[59] Kamide, K. and Sugamiya, K. (1970). *Makromol. Chem.*, **139**, 197.
[60] Kamide, K. and Sugamiya, K. (1972). *Makromol. Chem.*, **156**, 259.
[61] Kamide, K., Sugamiya, K., Terakawa, T., and Hara, T. (1972). *Makromol. Chem.*, **156**, 287.
[62] Kamide, K. and Yamaguchi, K. (1973). *Makromol. Chem.*, **167**, 287.
[63] Kamide, K., Miyazaki, Y., and Sugamiya, K. (1973). *Makromol. Chem.*, **173**, 113.
[64] Kamide, K., Yamaguchi, K., and Miyazaki, Y. (1973). *Makromol. Chem.*, **173**, 133.
[65] Kamide, K., Miyazaki, Y., and Yamaguchi, K. (1973). *Makromol. Chem.*, **173**, 153.
[66] Kamide, K., Miyazaki, Y., and Yamaguchi, K. (1973). *Makromol. Chem.*, **173**, 175.
[67] Kamide, K. and Miyazaki, Y. (1975). *Makromol. Chem.*, **176**, 1029.
[68] Kamide, K. and Miyazaki, Y. (1975). *Makromol. Chem.*, **176**, 1051.
[69] Kamide, K. and Miyazaki, Y. (1975). *Makromol. Chem.*, **176**, 1427.
[70] Kamide, K. and Miyazaki, Y. (1975). *Makromol. Chem.*, **176**, 1447.
[71] Kamide, K., Miyazaki, Y., and Abe, T. (1976). *Makromol. Chem.*, **177**, 485.
[72] Kamide, K., Miyazaki, Y., and Abe, T. (1981). *Brit. Polym. J.*, **13**, 168.
[73] Flory, P. J. (1953). *Principles of Polymer Chemistry*, Cornell University Press, Ithaca, NY, ch. 12.